The Canadian Mineralogist
Vol. 36, pp. 511-524 (1998)

A MICROBEAM XAFS STUDY OF AQUEOUS CHLOROZINC COMPLEXING TO 430°C IN FLUID INCLUSIONS FROM THE KNAUMÜHLE GRANITIC PEGMATITE, SAXONIAN GRANULITE MASSIF, GERMANY

ALAN J. ANDERSON[1]

Department of Geology, St. Francis Xavier University, P.O. Box 5000, Antigonish, Nova Scotia B2G 2W5

ROBERT A. MAYANOVIC

Department of Physics and Astronomy, Southwest Missouri State University, Springfield, Missouri 65804, U.S.A.

SAŠA BAJT[2]

Center for Advanced Radiation Sources, The University of Chicago, Chicago, Illinois 60637, U.S.A.

Abstract

The synchrotron X-ray microprobe (X26A) at the National Synchrotron Light Source (NSLS), Brookhaven National Laboratory was used to collect zinc *K*-edge absorption spectra from saline (*ca.* 36 wt% NaCl equiv.) fluid inclusions in quartz from the Knaumühle granitic pegmatite, in the Saxonian Granulite Massif, Germany, at temperatures ranging between 30° and 430°C. XAFS spectra were also obtained from one fluid inclusion that was experimentally re-equilibrated at a high pressure of hydrogen. The temperature of the fluid inclusions was controlled during analysis with a programmable heating stage. Analysis of the XAFS data shows that $ZnCl_4^{2-}$ is the dominant aqueous zinc species in the fluid inclusions up to the average trapping temperature (430°C). Furthermore, the mean Zn–Cl bond length decreases uniformly from 2.31 ± 0.01 Å at room temperature to 2.26 ± 0.02 Å at 430°C. The predominance of the tetrahedral chlorocomplex, rather than $ZnCl_2^0$, at high temperatures is most probably due to the high chloride concentrations of the inclusion brine.

Keywords: fluid inclusion, X-ray absorption fine structure, metalliferous brine, chlorozinc complex, granitic pegmatite, synchrotron X-ray microprobe, synchrotron X-ray fluorescence, hydrothermal fluid.

Sommaire

La microsonde X (X26A) à rayonnement synchrotron située au National Synchrotron Light Source (NSLS), Brookhaven National Laboratory a été utilisée pour obtenir des spectres d'absorption X au seuil *K* du zinc dans les inclusions fluides salines (environ 36% NaCl equivalents, en poids) dans le quartz provenant de la pegmatite granitique de Knaumühle, dans le massif granulitique de Saxe, en Allemagne, à des températures allant de 30° à 430°C. Des spectres XAFS ont aussi été obtenus dans le cas d'une inclusion fluide que nous avons ré-équilibré à pression élevée d'hydrogène. La température des inclusions fluides a été maintenue pendant l'analyse grâce à une platine chauffante programmable. Une analyse des données XAFS montre que le complexe $ZnCl_4^{2-}$ est dominant comme espèce aqueuse de zinc dans les inclusions fluides jusqu'à la température moyenne de piégeage, 430°C. De plus, la longueur moyenne de liaison Zn–Cl diminue de façon uniforme, de 2.31 ± 0.01 Å à température ambiante jusqu'à 2.26 ± 0.02 Å à 430°C. La prédominance du complexe tétraédrique chloré, plutôt que $ZnCl_2^0$, à température élevée, serait probablement due aux teneurs élevées de chlore dans la saumure piégée dans ces inclusions.

(Traduit par la Rédaction)

Mots-clés: inclusion fluide, structure fine de l'absorption X, saumure métallifère, complexe à chlorozinc, pegmatite granitique, microsonde X à rayonnement synchrotron, fluorescence X à rayonnement synchrotron, fluide hydrothermal.

[1] *E-mail address*: aanderso@stfx.ca
[2] Present address: Lawrence Livermore National Laboratory, P.O. Box 808, L-395, Livermore, California 94550, U.S.A.

INTRODUCTION

Knowledge of the speciation and structure of aqueous metal complexes at elevated temperatures is requisite for a complete understanding of the transport and deposition of ore metals in hydrothermal systems associated with igneous intrusions (Helgeson 1964, Barnes 1979, Crerar *et al.* 1985). Studies of fluid inclusions have shown that the fluids derived from shallow silicic intrusions are usually hypersaline (Roedder 1992, Cline & Bodnar 1991) and commonly contain high concentrations of metals such as Mn, Fe, Cu, Zn and Pb (Anderson *et al.* 1989, Heinrich *et al.* 1992). The stability of aqueous metallic species in chloride-rich hydrothermal fluids has been the focus of extensive research (Barnes 1979, Seward 1981); however, our understanding of metal complexing in highly saline fluids at temperatures above 350°C remains vague (Hemley *et al.* 1992, Cygan *et al.* 1994, Heinrich *et al.* 1996). This problem is due in part to the lack of solubility data from experiments conducted at total chloride concentrations greater than 6 molal (*i.e.*, 26 wt% NaCl) (Wood 1995).

Provisional estimates of the structure of concentrated aqueous alkali metal halide solutions at supercritical conditions have recently been made by Oelkers & Helgeson (1993) using Monte Carlo simulations. They suggested that polyatomic clusters become dominant in concentrated electrolyte solutions and that this significantly affects mineral solubilities as well as the thermodynamic properties of the fluid. Consequently, the practice of calculating solute speciation in high-salinity fluids by extrapolation of results from experiments on dilute electrolyte solutions may not be valid. Using X-ray and Raman scattering measurements at 25°C on zinc chloride hydrate melts, Yamaguchi *et al.* (1989) have noted that polymerization of tetrahedrally coordinated species occurs in solutions of concentrations of solute above 10 M.

Various spectroscopic techniques have been used to directly investigate solution speciation at elevated temperatures (*e.g.*, Franck 1973, Buback 1981, Seward 1984, Susak & Crerar 1985). One of the more important recent developments has been the application of X-ray Absorption Fine Structure (XAFS) to measurement of ion hydration in high-temperature solutions (Pfund *et al.* 1994, Fulton *et al.* 1996, Seward *et al.* 1997). Anderson *et al.* (1995) demonstrated the potential of microbeam XAFS for determining the structure of metal complexes within individual fluid inclusions at room temperature. In the present communication, we present the results of the first XAFS investigation of aqueous metallic species in high-salinity brine in single fluid inclusions at elevated temperatures, and extend the preliminary report of our study presented elsewhere (Mayanovic *et al.* 1996).

The fluid inclusions selected for analyses occur in quartz crystals from a vug in the Knaumühle pegmatite in the Saxonian Granulite Massif, Germany (Fig. 1). Similar granitic pegmatites have been described elsewhere in the region (Nurse 1993) and are associated with polymetallic sulfide hydrothermal veins that contain sphalerite (Neumann & Tischendorf 1986). The presence of coexisting vapor-rich inclusions and brine inclusions in the pegmatitic quartz indicate entrapment of a two-phase fluid. The analyses of high-temperature XAFS data from the highly saline aqueous inclusions show that a tetrahedral chlorozinc complex is dominant in the fluid inclusions up to the temperature of trapping, and that there is a progressive decrease in the Zn–Cl bond length with increasing temperature. The available compositional and microthermometric data on fluid inclusions from the nearby hydrothermal veins (Anderson *et al.* 1997) suggest that boiling, dilution and interaction with an external reduced sulfur species contributed to the destabilization of the zinc complex and the precipitation of sphalerite in the quartz veins.

GENERAL GEOLOGY

The samples used in this study were obtained from a vug in a pegmatite in the Grimmscher granulite quarry, at a location known as Knaumühle in the Saxonian Granulite Massif (Fig. 1). Both simple abyssal pegmatites and complex rare-element pegmatites occur in Proterozoic leucogranulites. The granulites are composed of quartz, mesoperthitic orthoclase and almandine, with subordinate amounts of kyanite, sillimanite, oligoclase, rutile, corundum and hercynitic spinel.

The pegmatites at Knaumühle consist mainly of K-feldspar, quartz and biotite. Large crystals of cordierite (up to 10 cm) are dispersed in the wall zone. The border zone contains cordierite and andalusite crystals up to 5 cm in length. Enrichment of lithium, boron and fluorine in some of the more evolved pegmatites is indicated by the presence of lepidolite, tourmaline (variety elbaite) and dumortierite. The rare-element pegmatites may be related to the nearby 350 ± 5 Ma Mittweida monzogranite (Fig. 1).

In the Hartmannsdorf quarry (12 km northwest of Chemnitz; Fig. 1), granitic pegmatites are spatially associated with hydrothermal veins and stringers that consist of quartz, calcite and a complex association of sulfides and sulfosalts. Jamesonite ($Pb_4FeSb_6S_{14}$) is the dominant sulfosalt in the veins, with minor amounts of arsenopyrite, löllingite, pyrite, cassiterite, sphalerite, chalcopyrite, boulangerite, tetrahedrite and gold (Neumann & Tischendorf 1986). According to these authors, the hydrothermal veins are a continuation of pegmatite mineralization.

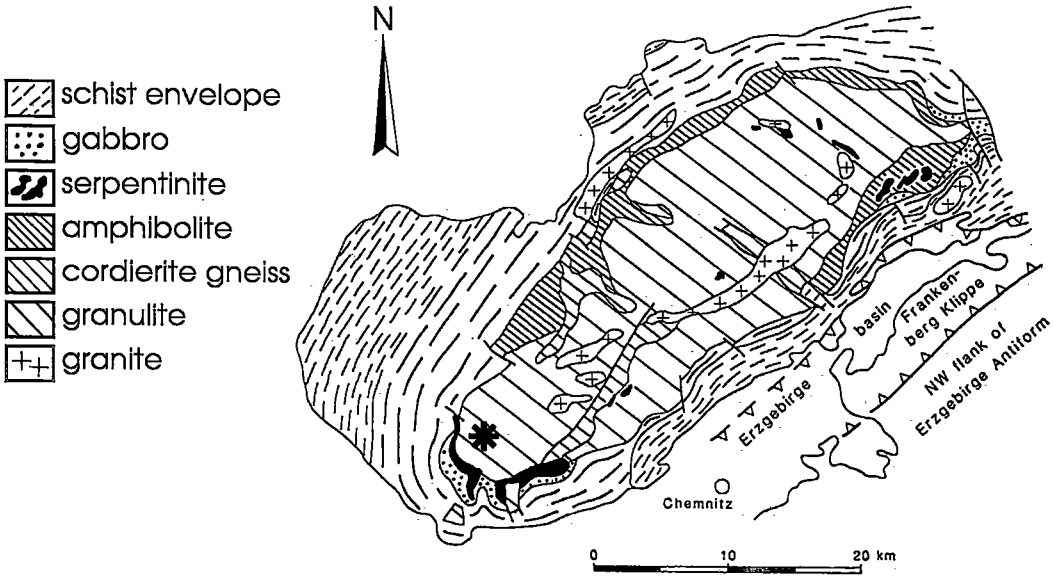

FIG. 1. Geological map of the Saxonian Granulite Massif, Germany, modified after Franke (1993). The asterisk designates the location of the granitic pegmatite sampled in this study.

EXPERIMENTAL METHODS

Fluid inclusion petrography and microthermometry

Two types of fluid inclusions were observed in doubly polished wafers prepared from the quartz crystal. These are: 1) high-salinity brine inclusions, which at room temperature consist of a metal-rich aqueous solution, a vapor bubble, and an assemblage of daughter minerals including halite and a high-birefringence Fe-rich phase (Fig. 2), and 2) vapor-rich inclusions which consist mainly of CO_2 with minor N_2, as indicated laser Raman micro-analysis (R. Thomas, pers. commun.). In some cases, the type-1 fluid inclusions may contain sylvite, calcite, wavellite and one or more unidentified phases. Both the brine- and vapor-rich inclusions attain 150 μm in their maximum dimension, and occur within healed microfractures. The ratio of phases in type-1 inclusions within a single fracture-plane appears to be nearly constant. In general, an individual fracture trapped either brine or vapor-rich fluid inclusions. Less commonly, however, both types of inclusions occur within the same fracture-plane, indicating entrapment of a two-phase fluid.

Volumes of fluid inclusions, and their depths beneath the polished surface of the quartz wafer, were obtained using a modified spindle stage (Anderson 1996) and a BIOQUANT OS/2 image analysis system at St. Francis Xavier University. Depth and volume measurements were necessary for selection of suitably large, near-surface fluid inclusions, and for calculation of metal concentrations from X-ray fluorescence yields.

Microthermometric data were obtained using a Linkham THMSG 600 programmable heating and freezing stage that was calibrated using synthetic fluid inclusion standards and the quartz α–β transition temperature. Apparent salinities of type-1 fluid inclusions were estimated from the temperature of halite dissolution using the equation of Chou (1987), and the temperatures of trapping were directly determined from the homogenization temperatures of cogenetic brine and vapor-rich inclusions.

Synchrotron X-ray-fluorescence microprobe analysis

Synchrotron X-ray-fluorescence (SXRF) spectra were collected from individual fluid inclusions using the X-ray microprobe X26A at the National Synchrotron Light Source (NSLS), Brookhaven National Laboratory, New York. Closely spaced tantalum slits were used to collimate the X-ray beam to an incident-beam spot size of 12 × 9 μm. The inclusions were excited by a chromatic (continuum energy spectrum) beam covering the range of 3–30 keV. The X-ray fluorescence signal from fluid inclusions was collected in air using a Si(Li) energy-dispersion detector positioned at 90° to the incident beam. X-ray maps of individual inclusions

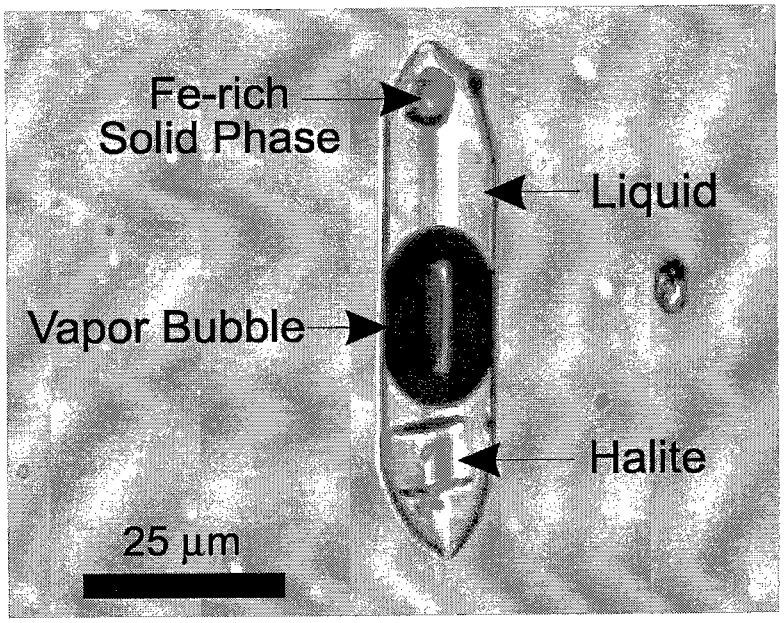

FIG. 2. Type-1 high-salinity fluid inclusion in quartz from the pegmatite.

were obtained by scanning the beam over the entire inclusion in 10 µm steps in both the *X* and *Y* directions. These maps were used to determine the distribution of Fe, Zn, Pb and Br within a single fluid inclusion. Additional details on the synchrotron X-ray fluorescence microprobe at the National Synchrotron Light Source (NSLS) can be found in Rivers *et al.* (1991).

Scanning electron microscopy – energy-dispersion analysis (SEM–EDA)

The SEM–EDA technique (Haynes *et al.* 1988) was useful for partial analysis for light elements (*Z* between 5 and 18) that could not be detected by *in situ* X-ray microprobe analysis of the fluid inclusions. Thin precipitates of salt on the polished surface of quartz, directly above thermally decrepitated fluid inclusions, were analyzed using an Electroscan Environmental Scanning Electron Microscope at the Bedford Institute of Oceanography, Dartmouth, Nova Scotia. Spectra were collected in the scanning and point modes at an accelerating voltage of 20 kV using a Si(Li) energy-dispersion spectrometer with an ultrathin (0.3 nm thick) Novar polymer window. Data obtained from opened fluid inclusions are qualitative owing to uncertainties resulting from preferential loss of volatile species at the time of thermal decrepitation.

Equilibration of fluid inclusions at high pressures of hydrogen

High hydrogen fugacities were generated in type-1 fluid inclusions in two quartz wafers prior to XAFS analysis in order to assess the possible effects of varying $f(H_2)$ on zinc speciation in the inclusion brines. Two polished sections of quartz containing type-1 fluid inclusions were placed in a gold capsule (25 mm length, 4.4 mm OD, 4.0 mm ID) containing CrN (from K & K Lab. Inc.) and H_2O. The capsule was sealed using an arc welder and then weighed before placing it into a cold-sealed pressure vessel fabricated from Stellite 25 alloy (from Haynes Stellite Co.). The vessel was pressurized by CH_4 and held at 2 kbar and 600°C for a period of six days. The total pressure of the vessel was maintained for the duration of the run by daily replenishment of CH_4 to compensate for the hydrogen lost through the wall of the pressure vessel. A high hydrogen pressure was generated within the gold capsule by the reaction of CrN with H_2O at 600°C, and by the use of the graphite–methane buffer, which significantly reduced the hydrogen fugacity gradient across the gold capsule wall. At 600°C, hydrogen within the capsule will readily diffuse through the quartz and into the fluid inclusions, as observed by Mavrogenes & Bodnar (1994) in a similar experiment.

After six days, the pressure vessel was removed from the furnace and cooled slowly to room temperature. The gold capsule was then extracted from the pressure vessel, dried, and weighed a second time to ensure that leakage had not occurred during the run. The polished wafers were then removed from the capsule and washed.

Collection of XAFS data

Temperature-dependent Zn *K*-edge XAFS spectra were collected in the fluorescence mode from individual fluid inclusions situated between 10 and 20 μm below the polished surface of the quartz wafer. XAFS spectra were also obtained at 400°C from a fluid inclusion that was re-equilibrated at high hydrogen pressures (see above).

Electrons within the NSLS X-ray storage ring were maintained at beam current levels ranging between 130 to 230 mA, at 2.54 GeV. The X26A beam line setup used to make the XAFS measurements is as follows: a white synchrotron X-ray beam entering from the front end of the beam line was made monochromatic (4–20 keV range) using a single Si(111) channel-cut crystal and focused with a 8:1 ellipsoidal Al (Pt coated) mirror, giving a flux of ~1×10^5 photons/s at 230 mA of stored current. The energy resolution using this setup was 1.5–2 eV. Harmonic rejection was accomplished with the focusing mirror, since it has an energy cutoff of roughly 14 keV. The 30 mm² Si(Li) energy-dispersion detector was used to collect the X-ray fluorescence signal in air. A pair of parallel 15-cm-long metal plates, set 1 cm apart, were positioned near the back end of the He-filled beam pipe. The detection of the ionization of He by X-rays passing through the gap between the plates was used to measure the intensity of the incident beam (I_0).

During XAFS measurement, the temperature of the fluid inclusion was controlled using a modified Linkham THMSG 600 programmable heating stage, which was mounted on the *X–Y–Z–*θ positioning stage of beam line X26A. The surface of the quartz wafer was precisely positioned using the *X–Y–Z–*θ stage and an optical microscope to give a 45° orientation to both the incident X-ray beam and the detector. In order to optimize the fluorescence yield, the size of the X-ray beam spot (as measured on the sample) was adjusted, using fine collimating slits and a pinhole mask, to the approximate dimensions of the fluid inclusion (*i.e.*, 60 × 24 μm). XAFS spectra were measured from the inclusion at temperatures ranging from 25 to 430°C (±1°C).

XAFS spectra were also measured at room temperature from standard zinc chloride (± sodium chloride) solutions having a chloride to zinc ratio between 2 and 8. The preparation of the solutions was described in Anderson *et al.* (1995). The solutions were inserted into plexiglass sample containers with thin Kapton windows in the walls to permit the transmission of both the incident X-ray beam and the resultant fluorescence X-rays. Three sets of XAFS spectra were obtained from the standard solutions and from the fluid inclusion at each temperature interval.

TABLE 1. THE Zn–Cl BOND LENGTH (R_{Zn-Cl}), COORDINATION NUMBER (N_{Cl}), AND MEAN-SQUARE RELATIVE DISORDER (σ^2) RESULTS, AND THE WINDOW RANGES FOR CALCULATION OF FOURIER TRANSFORMS (k-RANGE) AND THE FITTING RANGES (R-RANGE) FOR THE XAFS SPECTRA MEASURED BETWEEN 25° AND 430°C

T °C	R_{Zn-Cl} Å	N_{Cl}	σ^2 Å²	k-range Å⁻¹	R-range Å
25	2.30 ± 0.01	4.0 ± 0.4	0.0043 ± 0.0004	3.5–8.0	1.0–2.4
170	2.29 ± 0.01	3.8 ± 0.6	0.0064 ± 0.0005	2.8–8.75	1.4–2.15
250	2.29 ± 0.02	4.0 ± 0.4	0.0066 ± 0.0005	2.7–9.5	0.65–2.15
300	2.28 ± 0.01	4.1 ± 0.4	0.0070 ± 0.0006	2.9–9.3	0.65–2.25
430	2.26 ± 0.02	4.1 ± 0.5	0.0089 ± 0.0007	2.8–9.3	1.2–2.15

Analysis of XAFS data

Data analysis was made using the University of Washington software package (UWXAFS, version 2.01) according to the principles outlined by Sayers & Bunker (1988). Isolated oscillations (χ) of the XAFS data were produced by removing the pre-edge background using a simple second-order polynomial fit and by removing the above-edge background using a cubic least-squares-spline approximant over the 28–340 eV range. Fourier transforms were calculated from the $k^2\chi$ data using a modified Hanning function-type window over the k-ranges shown in Table 1. Quantitative structural information for the Zn environment was derived using theoretical spectra generated with FEFF 6 (Zabinsky *et al.* 1995, Mustre de Leon *et al.* 1991). The reader is referred to Anderson *et al.* (1995) for an explanation of the advantages of the XAFS technique for structural analysis of the aqueous species in fluid inclusions. Additional details on data collection and analysis are given in Mayanovic *et al.* (1996).

RESULTS

Microthermometry

Figure 3 shows the range of liquid–vapor homogenization temperatures (Th_{L-V}) *versus* the temperature of halite dissolution (Tm_{NaCl}) for high-salinity (type-1) fluid inclusions. The Th_{L-V} values for these inclusions average 90°C higher than the melting temperature of halite, and are therefore suitable for determination of apparent salinity using the temperature of halite dissolution, Tm_{NaCl}. Assuming a simple H_2O–NaCl

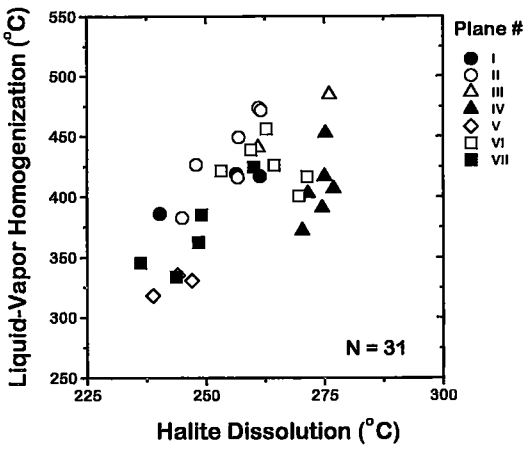

FIG. 3. Temperature of halite dissolution *versus* liquid–vapor homogenization temperature for type-1 fluid inclusions. The filled and solid symbols designate brine inclusions that belong to separate fluid-inclusion-decorated planes I to VII.

system, Tm_{NaCl} yields apparent salinities between 33 and 37 wt.% NaCl equivalent.

The Th_{L-V} for type-1 fluid inclusions is between 320 and 480°C. However, fluid inclusions trapped within a single healed fracture show a more restricted range of temperatures (Fig. 3), indicating different "closure temperatures" for different microfractures. The occurrence of brine and vapor-rich inclusions within the same healed fracture is evidence of entrapment of fluid in the two-phase (liquid + vapor) field. Therefore the temperature of homogenization is assumed to be the temperature of trapping, with no pressure correction required (Roedder 1984).

Using a temperature of trapping of 480°C (*i.e.*, the maximum homogenization temperature) and an average salinity of 35 wt.% NaCl equivalent, an estimated pressure of trapping of about 0.5 kbar is obtained using the vapor pressure curves for H_2O–NaCl solutions having salinities from 30 to 70 wt% NaCl of Bodnar & Vityk (1994). This is regarded as a minimum estimate of pressure because it does not account for the presence of CO_2, which significantly increases the T–P range of immiscibility.

Elemental analysis of fluid inclusions

Figure 4a shows a typical SEM–EDS spectrum obtained from salt precipitates on the quartz surface directly above a thermally decrepitated type-1 fluid inclusion. The SEM–EDS results consistently show the presence of Na, Cl, K, Mn, Fe and Zn; sulfur was not detected in any of the precipitates. The Si$K\alpha$ peak is generated from the quartz wafer. Figure 4b shows a synchrotron X-ray fluorescence spectrum obtained from an unopened type-1 fluid inclusion. The spectrum reveals relatively high concentrations (×1,000 ppm) of Mn, Fe, Zn, Br, Sb and Pb. The estimated average concentration of zinc in this inclusion is 0.4 wt%. Argon $K\alpha$ and Ti$K\alpha$ peaks are from the air and quartz, respectively. Na, Cl and K were not detected by SXRF owing to attenuation of their signal by the overlying quartz.

Zn K-edge XAFS measurements

The X-ray absorption coefficient at the Zn *K*-edge for standard solutions and a type-1 inclusion over a range of temperatures is shown in Figure 5. The temperature at which each spectrum was collected is shown with each spectrum. Figure 6 shows the isolated extended XAFS ($k^2\chi$) data of the Zn *K*-edge spectra in Figure 5.

Fourier transforms calculated from the $k^2\chi$ data are shown as points in Figure 7. The solid lines in Figure 7 represent the best-fit using FEFF 6 calculations

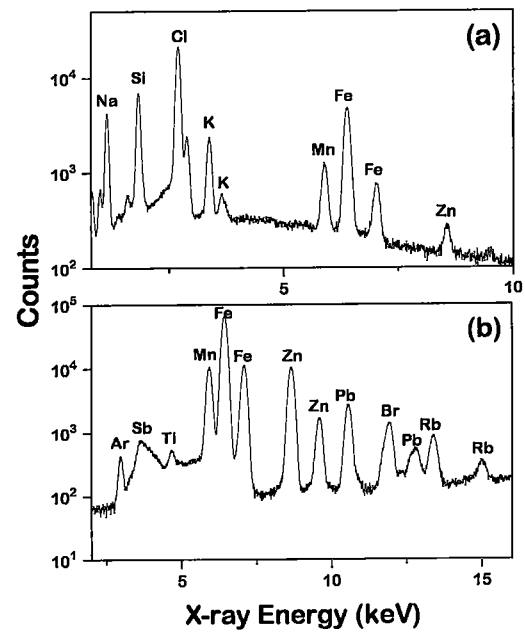

FIG. 4. (a) A typical energy-dispersion spectrum from an evaporite produced by thermal decrepitation of a type-1 fluid inclusion. (b) A synchrotron X-ray-fluorescence (SXRF) spectrum collected from a type-1 fluid inclusion such as in Figure 2.

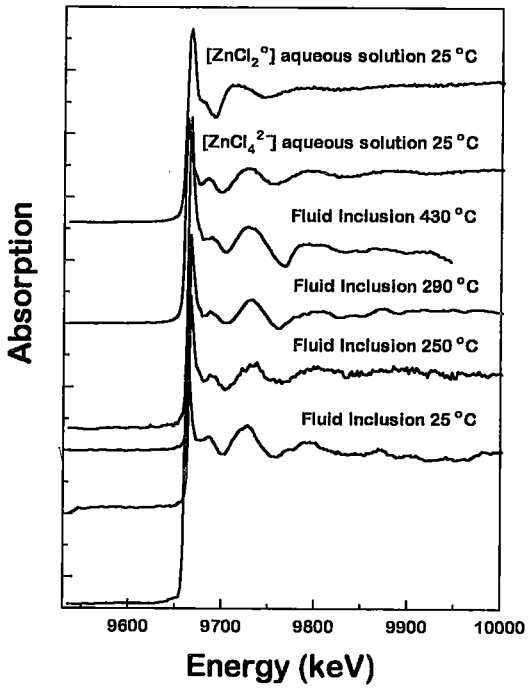

FIG. 5. Zn *K*-edge XAFS spectra collected in the fluorescence mode from a type-1 fluid inclusion at temperatures ranging from 25 to 430°C. Also shown are Zn *K*-edge XAFS spectra collected at room temperature from zinc chloride ($ZnCl_4^{2-}$) and ($ZnCl_2^0$) aqueous solutions.

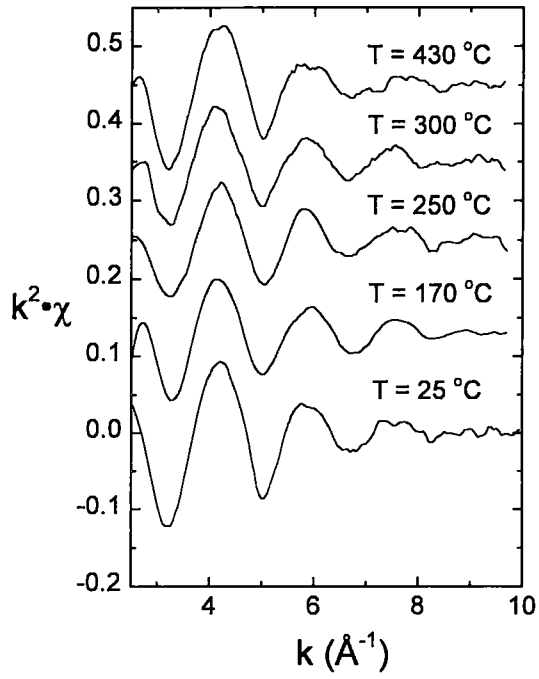

FIG. 6. The isolated extended XAFS ($k^2\chi$) of the Zn *K*-edge XAFS spectra shown in Figure 5.

assuming a $ZnCl_4^{2-}$ model. The Fourier transforms of the XAFS data are in excellent agreement with the theoretically generated results, indicating that the dominant aqueous zinc species in the inclusion brine up to 430°C is $ZnCl_4^{2-}$. This conclusion is supported by the close correlation between the XAFS spectra obtained from the fluid inclusion and those from the standard solution containing $ZnCl_4^{2-}$ (Fig. 5). Identical XAFS spectra were also collected at 400°C from a type-1 fluid inclusion that was re-equilibrated at high $f(H_2)$ conditions, indicating the predominance of $ZnCl_4^{2-}$ in this brine even at artificially high hydrogen pressures.

Table 1 lists the Zn–Cl bond lengths (R_{Zn-Cl}), coordination number (N_{Cl}), and the mean-square relative disorder σ^2 (MSRD) for the dominant chlorozinc complex in the inclusion brine over a range of temperatures, as determined from the fitting of the Fourier transform data in R-space. The results show that the coordination number of about 4 is constant over the entire range of temperature. There is, however, a significant reduction observed in the Zn–Cl bond length with increasing temperature by nearly 0.01 Å per 100°C (Fig. 8).

DISCUSSION

Composition and origin of the fluids

The type-1 fluid inclusions are dominated by NaCl, KCl and $FeCl_2$, with lesser concentrations of Mn, Zn, Pb, Sb, Br and Rb. Laser Raman analyses show variable but low amounts of CO_2 in the type-1 fluid inclusions (Anderson *et al.* 1997). A significant difference in composition between the present fluid inclusions and the highly saline fluid inclusions in porphyry Cu systems is the relatively high concentrations of Sb and the low concentrations of Cu (below detection). Campbell (1995) noted that fluids derived from the Capitan pluton, New Mexico, were low in Cu, and suggested that little Cu was present in the melt at the time of fluid separation.

Both brine- and vapor-rich fluid inclusions occur within healed fractures and are therefore presumed to be pseudosecondary or secondary in origin. The high metal concentrations in the fluid (*i.e.*, Mn, Fe, Zn and Pb) are in broad agreement with theoretical and experimental predictions for chloride-rich brines that equilibrated with granitic melts at high temperatures

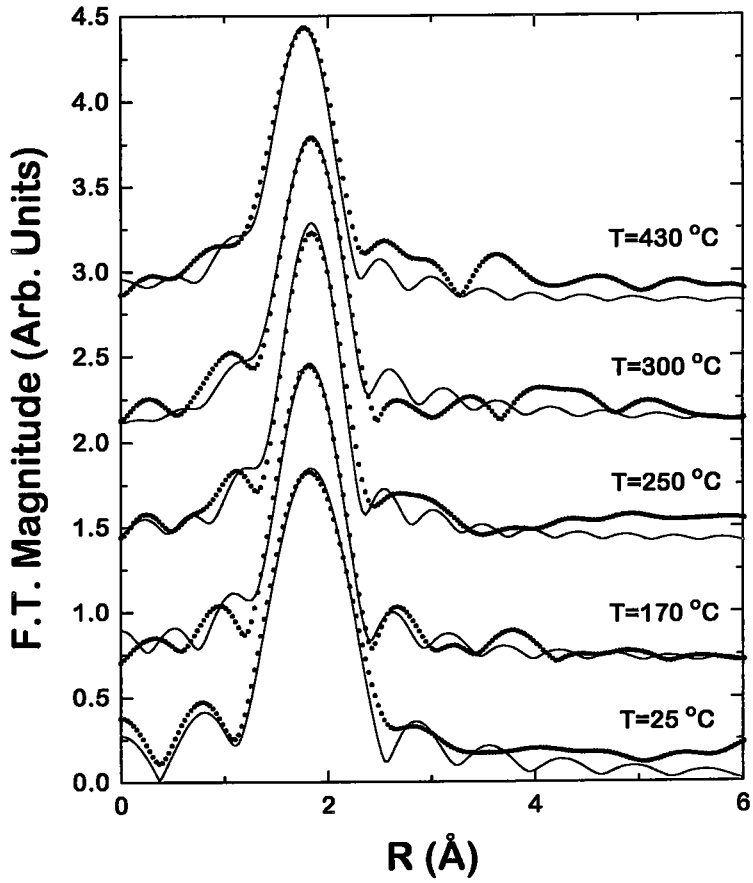

FIG. 7. The magnitude of the Fourier transform (FT) (dots) generated from the $k^2\chi$ data shown in Figure 6, and the best-fit model (solid lines) of these data using the program FEFF 6 and a $ZnCl_4^{2-}$ model.

(Eugster 1985, Whitney *et al.* 1985). Furthermore, the high concentrations Rb and Cs in the type-1 fluid inclusions (Anderson *et al.* 1997) is in agreement with fluid compositions associated with highly fractionated, rare-alkali-enriched pegmatite-forming melts (Lagache *et al.* 1995).

Secondary and pseudosecondary fluid inclusions of similar composition and filling temperatures have been described in other high-level granite–pegmatite systems (*e.g.*, Eadington 1983, Heinrich & Ryan 1992); these have been interpreted to be "near-pristine" samples of magmatic fluids. The high chloride concentrations in the present fluid inclusions relative to those found in spodumene-bearing pegmatites of the rare-element class may be due in part to the lower pressure at which the fluids were separated from the melt at near-solidus conditions (Cline & Bodnar 1991). Boiling also may have increased the salinity of the type-1 fluid inclusions. Aqueous fluid inclusions in spodumene-bearing rare-element pegmatites, such as at Tanco, Manitoba (London 1986), tend to have lower salinities (*ca.* 7 wt.% NaCl equiv.).

In some low-pressure systems, the final stages of pegmatite formation are marked by the separation of an aqueous fluid from the melt and the development of crystal-lined pockets and vugs. Subsequent "pocket rupture" (Jahns 1982) resulting in a sudden reduction in pressure may have induced microfracturing of the crystals and the unmixing of CO_2 from the fluid. Entrapment of brine- and vapor-rich inclusions by closure of the microcracks occurred over a temperature range of about 150°C (Fig. 3). The high concentrations

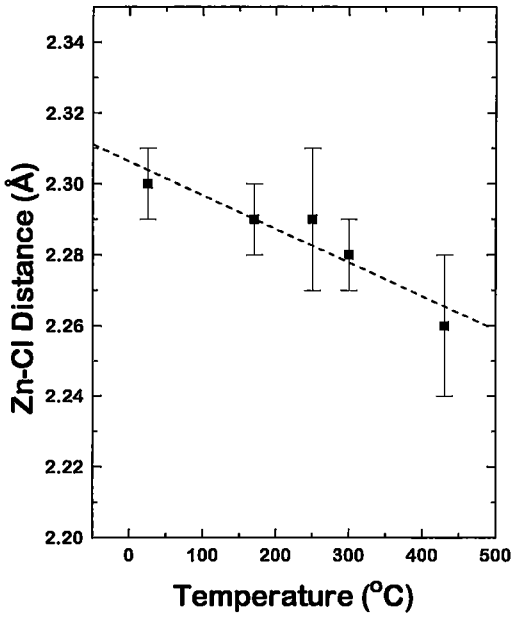

FIG. 8. Variation in the Zn–Cl bond length of the tetrahedral chlorozinc complex as a function of temperature. The dashed line is the linear fit of the data.

of Fe (percent level), Zn, Sb and Pb (several thousand ppm each) in the fluid inclusions favor a direct relationship between the pegmatites and the neighboring jamesonite-bearing quartz veins.

Neumann & Tischendorf (1986) proposed that the hydrothermal veins in the Hartmannsdorf quarry in the Saxonian Granulite Massif are a continuation of pegmatite mineralization, but suggested that the metals (*i.e.*, As, Zn, Fe, Sb, Pb) were mobilized from the surrounding host-rocks by retrograde processes of Variscan metamorphism. This interpretation is based in part on a Pb isotopic model age of 354 Ma obtained from jamesonite in the hydrothermal veins.

If the mineralized quartz veins are indeed a continuation of pegmatite mineralization as proposed by Neumann & Tischendorf, then it follows that the ore metals were derived from the pegmatite-forming melt, and not directly from the host granulites. In addition, it is unlikely that the formation of, and metal enrichment in, the rare-element-enriched pegmatite-forming melts is due to partial melting of a local granulite source-rock during metamorphism in view of the low pressures and temperatures indicated by the presence of: 1) cordierite and andalusite in the pegmatite (Černý & Hawthorne 1982), and 2) fluid inclusions trapped in the two-phase (liquid–vapor) field. The inferred conditions are insufficient for the generation of anatectic melts from granulite host-rocks.

In a study of sulfosalt-bearing veins of the Mid-European Saxothuringian zone, Dill (1985) rejected the genetic model invoking remobilization of metals from the enclosing country-rocks because the veins bearing the Pb–Sb sulfosalts cross-cut host rocks of different age and lithology and typically have Sn as a major trace element of the fahlores. Furthermore, Dill's Pb/Pb isotopic data suggest that the veins are related to calc-alkaline granites. On the basis of the composition of the fluid inclusions, we suggest that the fluids in the rare-element pegmatites at Knaumühle are genetically associated with the hydrothermal quartz veins of the region. The source and evolution of these hydrothermal fluids are the subject of a detailed study currently in progress (Anderson *et al.*, in prep.).

Zinc complexing in the hydrothermal fluids

Susak & Crerar (1985) have emphasized that knowledge of the molecular properties of hydrothermal fluids is essential to a complete understanding of mineral solubilities and hydrothermal processes. However, owing to experimental difficulties such as corrosion, there are essentially no experimental data available on metal complexing in high-temperature, high-salinity brines such as those associated with mineralized felsic intrusions (Roedder 1984). At

TABLE 2. CALCULATED AND EXPERIMENTAL BOND-LENGTHS FOR AQUEOUS ZINC-BEARING SPECIES AT ROOM TEMPERATURE

Species	Bond	Bond Length (Å) Calculated	Observed	Reference
$Zn(H_2O)_6^{2+}$	Zn–O	2.14		Parchment *et al.* (1996)
	Zn–O	2.09		Tossell (1990)
	Zn–O		2.08	Ohtaki *et al.* (1976)
$ZnCl^+$	Zn–Cl	2.08		Parchment *et al.* (1996)
	Zn–Cl	2.29		Tossell & Vaughan (1992)
	Zn–Cl		2.24	Maeda *et al.* (1996)
$ZnCl_2^0$	Zn–Cl	2.13		Parchment *et al.* (1996)
	Zn–Cl	2.21		Tossell & Vaughan (1992)
	Zn–Cl		2.24	Maeda *et al.* (1996)
$ZnCl_3^-$	Zn–Cl	2.26		Parchment *et al.* (1996)
	Zn–Cl	2.23		Tossell & Vaughan (1992)
	Zn–Cl		2.282(2)	Maeda *et al.* (1996)
$ZnCl_4^{2-}$	Zn–Cl	2.31		Tossell (1990)
	Zn–Cl	2.39		Parchment *et al.* (1996)
	Zn–Cl		2.28, 2.30	Kruh & Standley (1962)
	Zn–Cl		2.294(2)	Maeda *et al.* (1996)
$Zn(SH)_4^{2-}$	Zn–S	2.40		Tossell & Vaughan (1993)
$Zn(SH)_2Cl$	Zn–S	2.39		Tossell & Vaughan (1993)
	Zn–Cl	2.33		Tossell & Vaughan (1993)
	Zn–Cl		2.39	Helz *et al.* (1993)
$ZnBr_2^0$	Zn–Br		2.38	Dreier & Rabe (1986)
$Zn–Br_4^{2-}$	Zn–Br		2.41	Dreier & Rabe (1986)

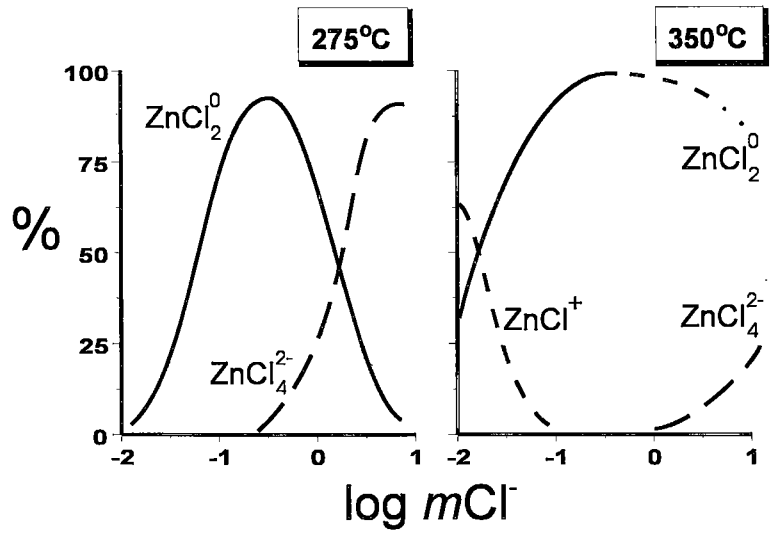

FIG. 9. The calculated preponderance of zinc species ($ZnCl_2^0$ and $ZnCl_4^{2-}$) in hydrochloric acid media at 275 and 350°C (after Ruaya & Seward 1986).

present, the most reliable data on aqueous species in hydrothermal solutions are biased toward low temperatures (*i.e.*, between 25 and 300°C) (Heinrich *et al.* 1996) and relatively low chloride concentrations (< 5 *m* Cl^-) (Wood 1995). Furthermore, most experimental studies involve relatively simple solutions that approximate natural hydrothermal fluids and thus do not take in to account the influence of minor components and various volatile species on solubilities of ore minerals (Walther & Schott 1988, Wood 1995).

The results presented here demonstrate that micro-beam XAFS analysis of highly saline natural and synthetic fluid inclusions at elevated temperatures can provide much needed data on metal speciation in brines of magmatic derivation. However, Hall *et al.* (1989), Morgan *et al.* (1993) and Sterner *et al.* (1995) have argued that natural fluid inclusions may undergo compositional re-equilibration after trapping, which may influence some aqueous species in the original entrapped fluid. Although it is generally accepted that the major constituents in fluid inclusions are preserved in most geological environments, there is strong evidence that hydrogen migrates in or out of fluid inclusions in quartz in response to a chemical potential gradient between the inclusions and an ambient fluid reservoir. Hydrogen loss from a fluid inclusion may influence the $f(O_2)$ and pH conditions of the original fluid. Roedder (1984) suggested that the presence of insoluble daughter minerals, such as chalcopyrite in fluid inclusions from porphyry copper deposits, is evidence that the original redox state of the fluid inclusion was modified by diffusion of hydrogen.

In order to assess the possible influence of natural loss of hydrogen on zinc speciation in the fluid inclusions studied, XAFS spectra were obtained from type-1 inclusions that were experimentally re-equilibrated at high hydrogen fugacities. The $f(H_2)$ in the experimentally re-equilibrated inclusions is, most probably, abnormally high relative to that in the original trapped fluid (Mavrogenes & Bodnar 1994). Nevertheless, the XAFS results show that the dominant zinc-bearing species in an inclusion subjected to high $f(H_2)$ is $ZnCl_4^{2-}$, which is identical to that in the untreated type-1 fluid inclusions. Although the actual $f(H_2)$ condition in the original fluid inclusion at the time of trapping is not known, there seems little doubt that the comparatively small changes in $f(H_2)$ expected to occur by natural diffusion of hydrogen would not influence the stability of chlorozinc species. Furthermore, the absence of insoluble solid phases and the dominance of aqueous Fe^{2+} in the fluid inclusions studied (Mayanovic & Anderson 1997) indicate that the original redox state of the entrapped fluid was not significantly modified, as is the case in many fluid inclusions from high-temperature porphyry systems.

Previous solubility studies predict that $ZnCl_2^0$ is the dominant zinc species at temperatures greater than 300°C for solutions in the 0.5 to 5.0 molal range of total chloride (Bourcier & Barnes 1987, Ruaya & Seward 1986, Cygan *et al.* 1994). The trend toward neutral-charge species is in agreement with a decrease in the dielectric constant of water with increasing temperature (Brimhall & Crerar 1987). However, for high-salinity fluids, such as in the present fluid inclu-

sions, models developed for relatively dilute aqueous solutions may not be valid, and very few experimental studies of solubility have been conducted at total chloride concentrations above 6 molal (Wood 1995).

The structure of aqueous chlorozinc complexes at room temperature has previously been investigated using XAFS, X-ray scattering, Raman and infrared measurements. Table 2 lists calculated and measured bond-lengths for various aqueous zinc species at room temperature. Although the tetrahedral zinc complex is dominant up to 430°C, the Zn–Cl bond lengths show a decrease of nearly 2% compared to the length at 25°C (Table 1). This real effect is evidenced in part by including the third- and fourth-order terms (C3 and C4, respectively) in the cumulant expansion in the fitting of the spectra, which may account for any anisotropy or anharmonicity in the radial distribution of the Cl ligand ions around the central zinc ion. It was found that these are very small; they were included in the fitting only for the two highest temperatures (*i.e.*, C3 = 3.8×10^{-4} Å^3 and C4 = 2.9×10^{-5} Å at 430°C). Simple calculations show that the increase in internal equilibrium pressure of the fluid inclusion can only account for 1 or 2% of the observed contraction in bond length with temperature.

Bond contraction may be associated with the progressive reduction of the dielectric constant of the fluid with increasing temperature. The combination of reduced hydrogen bonding and greater thermal agitation of water molecules causes a concomitant reduction of the solvent electric potential with temperature at the complex site. This reduction of the solvent potential should induce greater Zn–Cl electron orbital interaction at the complex site, which in turn would result in stronger and slightly contracted Zn–Cl bonds. The observed contraction of the bond and its effect on the stability of chloride complexes are the subjects of a parallel study that is currently in progress (Mayanovic *et al.*, in prep.).

Figure 9 shows the calculated distribution of $ZnCl_2^0$ and $ZnCl_4^{2-}$ in hydrochloric acid media at 275 and 350°C (after Ruaya & Seward 1986). At 350°C, Ruaya & Seward extrapolated the curves to Cl concentrations of 10 molal. In contrast to our XAFS results presented here, the extrapolated curves predict that $ZnCl_2^0$ is the dominant species at the chloride concentrations estimated in the inclusion brine (*ca.* 9 molal). It will be necessary to perform XAFS measurements on synthetic solutions having high Cl to Zn ratios at elevated temperatures in order to determine if the complex composition of the inclusion brine is responsible for the apparent enhanced stability of the tetrahedral zinc chlorocomplex.

The XAFS results indicate that a tetrahedral chlorozinc complex was the dominant species at the temperature of the fluid entrapment in the Knaumühle pegmatite. Fluid-inclusion and wallrock-alteration studies of the associated polymetallic sulfide-bearing quartz veins in the region are currently in progress to determine the factors controlling the destabilization of the tetrahedral chlorozinc complex and the precipitation of sphalerite.

Minimum detection-limits for XAFS analysis of fluid inclusions

The minimum detection-limit for a particular element within a fluid inclusion using XAFS is strongly controlled by sample parameters such as inclusion volume and its depth beneath the polished surface of the host mineral. Therefore, judicious choice of a large, near-surface fluid inclusion is required to optimize the X-ray fluorescence yield. At high temperatures, the XAFS spectra may be slightly dampened by atomic displacements due to thermal disorder (Crozier 1988). Nevertheless, this additional noise did not adversely affect data analyses in the present study. The sensitivity of the technique is also dependent on the atomic number of the absorbing ion. Relatively low-energy X-rays generated from light elements such as Na, Mg, K are severely attenuated by the host mineral, and are thus difficult to monitor. At present, the minimum detection-limit for XAFS analysis of fluid inclusions using the X-ray microprobe (X26A) at the National Synchrotron Light Source precludes investigation of a wide range of solutes that typically occur in low concentrations (<100 ppm) in hydrothermal solutions. We anticipate lower detection-limits by using brighter X-ray sources than are now available.

Conclusions

A full understanding of the macroscopic behavior of aqueous species in hydrothermal solutions can only be obtained from a detailed knowledge of their atomistic nature. We report the first XAFS study of metal complexing at elevated temperatures in natural fluid inclusions, before and after experimental re-equilibration at high fugacities of hydrogen. Our results indicate that the tetrahedral chlorozinc complex, $ZnCl_4^{2-}$, is the dominant aqueous zinc species at temperatures up to 430°C, and that there is a significant decrease in the length of the Zn–Cl bond with increasing temperature. These results suggest that zinc was transported as a tetrahedral chlorocomplex in the hydrothermal solutions that seem involved in the deposition of sulfide-bearing quartz veins in the region. The presence of the tetrahedral chlorozinc species in fluid inclusions that were experimentally re-equilibrated at high hydrogen pressures indicates that natural re-equilibration of $f(H_2)$ most probably did not influence the chlorozinc species in the fluid inclusions studied. XAFS analysis of natural fluid inclusions, such as those used in this study, provides the most direct evidence of metal complexing in paleohydrothermal solutions.

ACKNOWLEDGEMENTS

We are indebted to I-Ming Chou (U.S. Geological Survey) for experimentally re-equilibrating natural fluid inclusions at elevated pressures of hydrogen. Laser Raman analysis and information on the geology of the Saxonian Granulite Massif were kindly provided by Rainer Thomas (GeoforschungZentrum Potsdam). Frank Thomas and Kate Moran (Bedford Institute of Oceanography) are thanked for permission to use their Environmental Scanning Electron Microscope. Tracy Cail assisted with microthermometric measurements. The manuscript benefitted from reviews by Mike Fleet, Bob Martin, Skip Simmons and Al Falster. This study was supported by a NSERC research grant to A.J.A., DOE grant (DE–FGO2–92ER14244) to S.B. and DOE grant (DE–ACO2–76CHOOO16) to Brookhaven National Laboratory. We thank the NSLS staff for providing synchrotron radiation.

REFERENCES

ANDERSON, A.J. (1996): A new oil immersion vessel for optical spindle stage examination of fluid and solid inclusions. *In* PACROFI VI, Sixth biennial Pan-American Conf. on Research on Fluid Inclusions (Madison, Wisconsin; D.E. Brown & G.S. Hagemann, eds.), Program Abstr.

_____, CLARK, A.H., MA, XIN-PEI, PALMER, G.R., MACARTHUR, J.D. & ROEDDER, E. (1989): Proton-induced X-ray and gamma-ray emission analysis of unopened fluid inclusions. *Econ. Geol.* **84**, 924-939.

_____, MAYANOVIC, R.A. & BAJT, S. (1995): Determination of the local structure and speciation of zinc in individual hypersaline fluid inclusions by micro-XAFS. *Can. Mineral.* **33**, 499-508.

_____, _____, HORN, I., JACKSON, S. & THOMAS, R. (1997): Element partitioning and ore-metal transport in a two-phase hydrothermal system: evidence from fluid inclusions in pegmatites and associated polymetallic sulfide veins in the Saxonian Granulite Massif, Germany. *In* ECROFI XIV, European Current Research on Fluid Inclusions (Nancy, France), Abstr.

BARNES, H.L. (1979): Solubilities of ore minerals. *In* Geochemistry of Hydrothermal Ore Deposits (2nd edition; H.L. Barnes, ed.). Wiley-Interscience, New York, N.Y. (404-460).

BODNAR, R.J. & VITYK, M.O. (1994): Determination of fluid inclusion compositions. *In* Fluid Inclusions in Minerals: Methods and Applications (B. De Vivo & M.L. Frezzotti, eds.). Short Course of the IMA working group "Inclusions in Minerals" (Pontignano – Siena), 117-130.

BOURCIER, W.L. & BARNES, H.L. (1987): Ore solution chemistry. VII. Stabilities of chloride and bisulfide complexes of zinc to 350°C. *Econ. Geol.* **82**, 1839-1863.

BRIMHALL, G.H. & CRERAR, D.A. (1987): Ore fluids: magmatic to supergene. *In* Thermodynamic Modeling of Geological Materials: Minerals, Fluids and Melts (I.S.E. Carmichael & H.P. Eugster, eds.). *Rev. Mineral.* **17**, 235-321.

BUBACK, M. (1981): Spectroscopic investigations of fluids. *In* Chemistry and Geochemistry of Solutions at High Temperatures and Pressures (F.E. Wickman & D.T. Rickard, eds.). *Phys. Chem. Earth* **13-14**, 345-356.

CAMPBELL, A.R. (1995): The evolution of a magmatic fluid: a case history from the Capitan Mountains, New Mexico. *In* Magmas, Fluids, and Ore Deposits (J.F.H. Thompson, ed.). *Mineral. Assoc. Can., Short-Course Vol.* **23**, 139-152.

ČERNÝ, P. & HAWTHORNE, F.C. (1982): Selected peraluminous minerals. *In* Granitic Pegmatites in Science and Industry (P. Černý, ed.). *Mineral. Assoc. Can., Short-Course Handbook* **8**, 163-186.

CHOU, I-MING (1987): Phase relations in the system NaCl–KCl–H_2O. III. Solubilities of halite in vapor-saturated liquids above 445°C and redetermination of phase equilibrium properties in the system NaCl–H_2O to 1000°C and 1500 bars. *Geochim. Cosmochim. Acta* **51**, 1965-1975.

CLINE, J.S. & BODNAR, R.J. (1991): Can economic porphyry copper mineralization be generated by a "typical" calc-alkaline melt? *J. Geophys. Res.* **96**, 8113-8126.

CRERAR, D., WOOD, S.A., BRANTLEY, S. & BOCARSLY, A. (1985): Chemical controls on solubility of ore-forming minerals in hydrothermal solutions. *Can. Mineral.* **23**, 333-352.

CROZIER, E.D., REHR, J.J. & INGALLS, R. (1988): Amorphous and liquid systems. *In* X-ray Absorption, Principles, Applications, Techniques of EXAFS, SEXAFS and XANES (D.C. Koningsberger & R. Prins, eds.). John Wiley & Sons, New York.

CYGAN, G.L., HEMLEY, J.J. & D'ANGELO, W.M. (1994): An experimental study of zinc chloride speciation from 300 to 600°C and 0.5 to 2.0 kbar in buffered hydrothermal solutions. *Geochim. Cosmochim. Acta* **58**, 4841-4855.

DILL, H. (1985): Antimoniferous mineralization from the Mid-European Saxothuringian Zone: mineralogy, geology, geochemistry and ensialic origin. *Geol. Rundschau* **74**, 447-466.

DREIER, P. & RABE, P. (1986): EXAFS-study of the Zn^{2+} coordination in aqueous halide solutions. *J. Physique* **C8**, 809-812.

EADINGTON, P.J. (1983): A fluid inclusion investigation of ore formation in a tin-mineralized granite, New England, New South Wales. *Econ. Geol.* **78**, 1204-1221.

EUGSTER, H.P. (1985): Granites and hydrothermal ore deposits: a geochemical framework. *Mineral. Mag.* **49**, 7-23.

FRANCK, E.U. (1973): Concentrated electrolyte solutions at high temperatures and pressures. *J. Solution Chem.* **2**, 339-356.

FRANKE, W. (1993): The Saxonian granulites: a metamorphic core complex? *Geol. Rundschau* **82**, 505-515.

FULTON, J.L., PFUND, D.M., WALLEN, S.L., NEWVILLE, M., STERN E.A. & MA, YANJUN (1996): Rubidium ion hydration in ambient and supercritical water. *J. Chem. Phys.* **105**, 2161-2166.

HALL, D.L., STERNER, S.M. & BODNAR, R.J. (1989): Experimental evidence for hydrogen diffusion into fluid inclusions in quartz. *Geol. Soc. Am., Abstr. Program* **21**, A358.

HAYNES, F.M., STERNER, S.M. & BODNAR, R.J. (1988): Synthetic fluid inclusions in natural quartz. IV. Chemical analyses of fluid inclusions by SEM/EDA: evaluation of method. *Geochim. Cosmochim. Acta* **52**, 969-977.

HEINRICH, C.A. & RYAN, C.G. (1992): Mineral paragenesis and regional zonation of granite-related Sn–As–Cu–Pb–Zn deposits: a chemical model for the Mole Granite district (Australia) based on PIXE fluid inclusion analyses. *In* Proc. 7th Int. Symp. on Water–Rock Interaction **2** (Y.K. Kharaka & A.S. Maest, eds.). Balkema, Rotterdam, The Netherlands (1583-1587).

_____, WALSHE, J.L. & HARROLD, B.P. (1996): Chemical mass transfer modelling of ore-forming hydrothermal systems: current practise and problems. *Ore Geology Rev.* **10**, 319-338.

HELGESON, H.C. (1964): *Complexing and Hydrothermal Ore Deposition*. Pergamon, New York, N.Y.

HELZ, G.R., CHARNOCK, J.M., VAUGHAN, D.J. & GARNER, C.D. (1993): Multinuclearity of aqueous copper and zinc bisulfide complexes: an EXAFS investigation. *Geochim. Cosmochim. Acta* **57**, 15-25.

HEMLEY, J.J., CYGAN, G.L., FEIN, J.B., ROBINSON, G.R. & D'ANGELO, W.M. (1992): Hydrothermal ore-forming processes in the light of studies in rock-buffered systems. I. Iron–copper–zinc–lead sulfide solubility relations. *Econ. Geol.* **87**, 1-22.

JAHNS, R.H. (1982): Internal evolution of pegmatite bodies. *In* Granitic Pegmatites in Science and Industry (P. Černý, ed.). *Mineral. Assoc. Can., Short-Course Handbook* **8**, 293-327.

KRUH, R.F. & STANDLEY, C.L. (1962): An X-ray diffraction study of aqueous zinc chloride solutions. *Inorg. Chem.* **1**, 941-943.

LAGACHE, M., DUJON, S.-C. & SEBASTIAN, A. (1995): Assemblages of Li–Cs pegmatite minerals in equilibrium with a fluid from their primary crystallization until their hydrothermal alteration: an experimental study. *Mineral. Petrol.* **55**, 131-143.

LONDON, D. (1986): Magmatic–hydrothermal transition in the Tanco rare element pegmatite: evidence from fluid inclusions and phase-equilibrium experiments. *Am. Mineral.* **71**, 376-395.

MAEDA, M., ITO, I., HORI, M. & JOHANSSON, G. (1996): The structure of zinc-chloride complexes in aqueous solution. *Z. Naturforschung Section A-A Journal of Physical Sciences.* **51**, 63-70.

MAVROGENES, J.A. & BODNAR, R.J. (1994): Hydrogen movement into and out of fluid inclusions in quartz: experimental evidence and geologic implications. *Geochim. Cosmochim Acta* **58**, 141-148.

MAYANOVIC, R.A. & ANDERSON, A.J. (1997): Micro-beam XAFS studies on fluid inclusions under hydrothermal conditions. *In* ECROFI XIV, European Current Research on Fluid Inclusions (Nancy, France), Abstr. (203-204).

_____, _____ & BAJT, S. (1996): Microbeam XAFS investigations on fluid inclusions. *In* Applications of Synchrotron Radiation Techniques to Materials Science III (L.J. Terminello, S.M. Mini, H. Ade & D.L. Perry, eds.). *Materials Res. Soc., Symp. Proc. Vol.* **437**, 201-206.

MORGAN, G.B., VI, CHOU, I-MING, PASTERIS, J.D. & OLSEN, S.N. (1993): Re-equilibration of CO_2 fluid inclusions at controlled hydrogen fugacities. *J. Metamorphic Geol.* **11**, 155-164.

MUSTRE DE LEON, J., REHR, J.J., ZABINSKY, S.I. & ALBERS, R.C. (1991): *Ab initio* curved-wave X-ray-absorption fine structure. *Phys. Rev.* **B 44**, 4146-4156.

NEUMANN, W. & TISCHENDORF, G. (1986): Genesis of sulfide mineralization in pyriclasites of Hartmannsdorf, Granulite Massif. *In* Proc. Conf. Metallogeny of the Precambrian (Z. Pouba, ed.). *Int. Geol. Correlation Program, Project* **91**, 81-84.

NURSE, R.E.G. (1993): *Paragenetische und thermobarometrische Untersuchungen an strukturgebundenen Mineralisationen im Sächsischen Granulitgebirge*. Dissertation, Freiberg University of Mining and Technology, Freiberg, Germany.

OELKERS, E.H. & HELGESON, H.C. (1993): Multiple ion association in supercritical aqueous solutions of single electrolytes. *Science* **261**, 888-891.

OHTAKI, H., YAMAGUCHI, T. & MAEDA, M. (1976): X-ray diffraction studies of the structures of hydrated divalent transition-metal ions in aqueous solutions. *Bull. Chem. Soc. Japan* **49**, 701-708.

PARCHMENT, O.G., VINCENT, M.A. & HILLIER, I.H. (1996): Speciation in aqueous zinc chloride. An *ab initio* hybrid microsolvation/continuum approach. *J. Phys. Chem.* **100**, 9689-9693.

PFUND, D.M., DARAB, J.G., FULTON, J.L. & MA, YANJUN (1994): An XAFS study of strontium ions and krypton in supercritical water. *J. Phys. Chem.* **98**, 13102-13107.

RIVERS, M.L., SUTTON, S.R. & JONES, K.W. (1991): Synchrotron X-ray fluorescence microscopy. *Synchr. Rad. News* **4**, 23-26.

ROEDDER, E. (1984): Fluid inclusions. *Rev. Mineral.* **12**.

_____ (1992): Fluid inclusion evidence for immiscibility in magmatic differentiation. *Geochim. Cosmochim. Acta* **56**, 5-20.

RUAYA, J.R. & SEWARD, T.M. (1986): The stability of chlorozinc(II) complexes in hydrothermal solutions up to 350°C. *Geochim. Cosmochim. Acta* **50**, 651-661.

SAYERS, D.E. & BUNKER, B.A. (1988): Data analysis. *In* X-ray Absorption, Principles, Applications, Techniques of EXAFS, SEXAFS and XANES (D.C. Koningsberger & R. Prins, eds.). John Wiley & Sons, New York, N.Y.

SEWARD, T.M. (1981): Metal complex formation in aqueous solution at elevated temperatures and pressures. *In* Chemistry and Geochemistry of Solutions at High Temperatures and Pressures (F.E. Wickman & D.T. Rickard, eds.). *Phys. Chem. Earth* **13-14**, 113-129.

_____ (1984): The formation of lead(II) chloride complexes to 300°C: a spectrophotometric study. *Geochim. Cosmochim. Acta* **48**, 121-134.

_____, HENDERSON, C.M.B., CHARNOCK, J.M. & DOBSON, B.R. (1997): An X-ray absorption (EXAFS) spectroscopic study of aquated Ag^+ in hydrothermal solutions to 350°C. *Geochim. Cosmochim. Acta* **60**, 2273-2282.

STERNER, S.M., HALL, D.L. & KEPPLER, H. (1995): Compositional re-equilibration of fluid inclusions in quartz. *Contrib. Mineral. Petrol.* **119**, 1-15.

SUSAK, N.J. & CRERAR, D.A. (1985): Spectra and coordination changes of transition metals in hydrothermal solutions: implications for ore genesis. *Geochim. Cosmochim. Acta* **49**, 555-564.

TOSSELL, J.A. (1990): Ab initio calculation of the structures, Raman frequencies and Zn NMR spectra of tetrahedral complexes of Zn^{2+}. *Chem. Phys. Lett.* **169**, 145-149.

_____ & VAUGHAN, D.J. (1992): *Theoretical Geochemistry: Applications of Quantum Mechanics in the Earth and Mineral Sciences*. Oxford University Press, New York, N.Y.

_____ & _____ (1993): Bisulfide complexes of zinc and cadmium in aqueous solution: calculation of structure, stability, vibrational, and NMR spectra, and speciation on mineral surfaces. *Geochim. Cosmochim. Acta* **57**, 1935-1945.

WALTHER, J.V. & SCHOTT, J. (1988): The dielectric constant approach to speciation and ion pairing at high temperature and pressure. *Nature* **332**, 635-638.

WHITNEY, J.A., HEMLEY, J.J. & SIMON, F.O. (1985): The concentration of iron chloride solutions equilibrated with synthetic granitic compositions: the sulfur-free system. *Econ. Geol.* **80**, 444-460.

WOOD, S.A. (1995): Solubility constraints on the size of hydrothermal ore deposits. *In* Proc. Second Giant Ore Deposits Workshop, Controls on the Scale of Orogenic Magmatic–Hydrothermal Mineralization (A.H. Clark, ed.). QminEx Associates, Kingston, Ontario (262-299).

YAMAGUCHI, T., HAYASHI, S & OHTAKI, H. (1989): X-ray diffraction and Raman studies of zinc(II) chloride hydrate melts, $ZnCl_2.H_2O$ (R = 1.8, 2.5, 3.0, 4.0, and 6.2). *J. Phys. Chem.* **93**, 2620-2625.

ZABINSKY, S.I., REHR, J.J., ANKUDINOV, A., ALBERS, R.C. & ELLER, M.J. (1995): Multiple-scattering calculations of X-ray absorption spectra. *Phys. Rev.* **B52**, 2995-3009.

Received September 5, 1996, revised manuscript accepted February 2, 1998.